Aerodynamic Characteristics and Plasma Flow Control of Static Hysteresis over an Airfoil at Low Reynolds Numbers

Haoyu Chen[1], Long Zhou[2], and Xuanshi Meng[1(✉)]

[1] Department of Fluid Mechanics, Northwestern Polytechnical University,
Xi'an 710072, China
mxsbear@nwpu.edu.cn
[2] Department of Aerodynamics, Nanjing University of Aeronautics
and Astronautics, Nanjing 210016, China

Abstract. An experimental study is performed to characterize the static hysteresis of the lift and drag on an FX 63-137 airfoil at the chord Reynolds number of 1.8×10^5. A long strip of plasma actuator is installed on the upper surface near the leading edge of the airfoil. The purpose of this work is to study the effect of plasma flow control on the static hysteresis of lift and drag at low Reynolds numbers. Pressure measurements are used to determine the surface pressure distribution around the airfoil. Lift and drag forces acting on the airfoil are calculated from the measured pressures and normalized by the chord. The detailed surface pressure distributions over the baseline airfoil reveal that it is the laminar separation bubble (LSB) on the upper surface delays the stall for the forward process of the angles of attack (AOA); while for the backward process of AOA, the flow cannot establish the same laminar separation bubble as the forward process, resulting in the static hysteresis of the lift and drag. The plasma flow control results show that static hysteresis of lift and drag can be reduced by affecting the LSB at low Reynolds numbers.

Keywords: Low Reynolds number · Active flow control · Plasma ·
Lift and drag · Static hysteresis

1 Introduction

Recently aerodynamic problems at low Reynolds numbers have attracted aeronautical engineers' attention. There are various applications (such as unmanned aerial vehicles (UAVs), micro-mini drones, gliders, low-speed adjacent space vehicles, wind turbine blades, turbine blades, and compressors) at low Reynolds numbers in both civilian and military field, thus the study of low Reynolds number aerodynamic problems which need in-depth research becomes extremely important.

When Reynolds number is less than 200,000, there will be some significant aerodynamic phenomena, mainly as follows: For symmetrical airfoil, there is a non-linear change in lift with increasing angle of attack (AOA) at a small AOA range [1], for the high lift camber airfoil, static hysteresis of lift and drag occurs [15, 18], and lift-to-drag ratio is rapidly reduced [7]. These aerodynamic problems of low Reynolds

numbers are undesirable for aircraft design, especially static hysteresis of the lift and drag and rapid decrease of the lift-to-drag ratio, which may lead to operational delays and even flight accidents. Therefore, the mechanism of static hysteresis must be studied in depth and some flow control method should be taken to weaken or eliminate these phenomena.

A great deal of research has been done on these phenomena, and it has been found that these phenomena at low Reynolds numbers are closely related to the laminar flow separation. For the laminar separation phenomenon, Horton [6] proposed a separation bubble model. At low Reynolds numbers, because the existence of adverse pressure gradient, the separated boundary layer becomes unstable, and the transition will occur very quickly, as the flow becomes turbulent. If the turbulence can overcome the reverse pressure gradient, flow reattachment occurs, thus forming a separation bubble between the separation point and the reattachment point [2, 5, 10].

For the laminar separation phenomenon at low Reynolds number, Mcgranahan and Selig [12] carried out surface oil flow test and pressure measurement test on several typical airfoils, and analyzed the separation points, indicating the position of the oil flow accumulation line and the time-average line is a little different. Wu et al. [17] studied the flow characteristics of the NACA0012 airfoil at a Reynolds number of 8,200 through the oxygen bubble flow visualization and PIV test. The study found that the vortex formed at the separation point and the separated shear layer moves upstream with the increase of AOA, and the recirculation zone becomes larger as AOA increases.

Regarding the study of active or passive control of laminar flow separation, Chen et al. [3] used electromagnetic force to suppress flow separation. Liu et al. [9] performed a numerical simulation of flow separation under suction or blowing flow control. Moreover, a technique called plasma actuation flow control has received growing attention in recent years because of their advantages such as zero reaction time, broad frequency bandwidths, relatively low energy consumption, and conveniently installation [4, 8, 16].

The primary objective of the current work is to investigate the aerodynamic characteristics and the plasma flow control effects on static hysteresis of an FX 63-137 airfoil at the Reynolds number of 1.8×10^5. Pressure measurement test will be applied as a primary method.

2 Experimental Setup

2.1 Wind-Tunnel Facility and Model

The experiments are performed in a $1.0\,\text{m} \times 0.4\,\text{m}$ binary test section of the low-speed low-turbulence wind tunnel at Northwestern Polytechnical University. In this study, the free-stream velocity is set to $U_\infty = 15\,\text{m/s}$ with the chord Reynolds number of 1.8×10^5. The turbulence is about adjustable in a range of 0.02%–0.3% by changing the console numbers.

For the study of static hysteresis of an airfoil at low Reynolds numbers, the FX 63-137 airfoil is chosen as shown in Fig. 1. The FX 63-137 airfoil model is made of wood, whose thickness is of 14%, camber of 6%. The span of this model is 398 mm, and the

chord length is 200 mm. The machining error of this wooden model is 0.06 mm, which indicates that the model can be used in this experiment. There is white paint on the model surface to reduce friction, and there are 24 pressure taps on each side of the model. The model of pressure taps is 9816 by the PSI Company with an accuracy of up to ±0.05% FS, which are read at the frequency of 50 Hz. The airfoil model is carefully cleaned before each run of the wind tunnel.
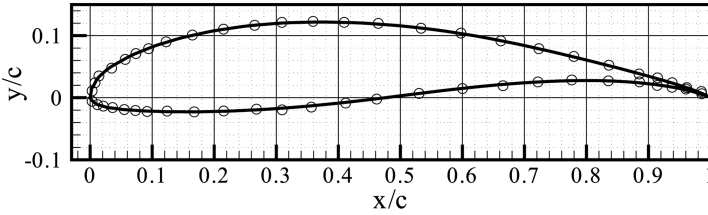
Fig. 1. FX 63-137 airfoil geometry and pressure tappings arrangements sketch

As shown in Fig. 2a, the pressure taps are distributed in the middle of the airfoil, and there is a wake rake with 60 total pressure and four static pressure probes locate at $0.9\,c$ downstream of the airfoil. The rake width is 300 mm which can adequately cover the entire wake field at all the test AOA range. The tubes shown in Fig. 2b are pressure tubes, through which the pressure taps are connected to a scanning valve, and the scanning valve is connected to the computer which could record pressure data. In this study, the AOA is set at $-10°–30°$, and the AOA change modes are defined. In the forward mode, the AOA increases from $-10°$ to $30°$, with a step of $2°$. In the backward mode, the AOA decreases from $30°$ to $-10°$, with a step of $-2°$.


| (a) | (b) |
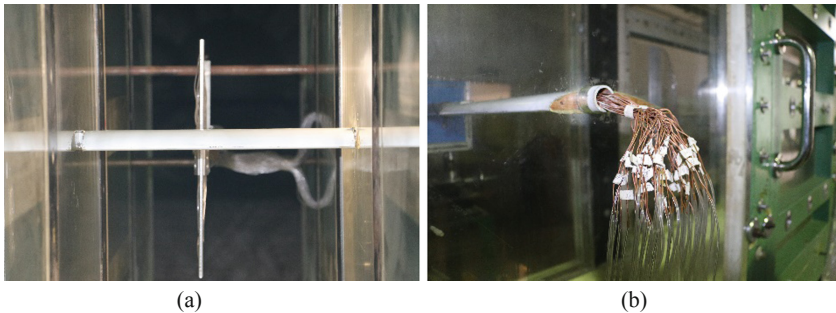
Fig. 2. Sketches of pressure measurement experiment layout and model configuration. (a) Pressure measurement experiment layout in wind tunnel. (b) Airfoil model and pressure tubes configuration

The pressure coefficient distributions, $C_p = (p - p_\infty)/(\frac{1}{2}\rho U_\infty^2)$, around the airfoil at various AOA and Reynolds numbers are measured by the pressure acquisition system described above. The lift coefficient $(C_L = L/(\frac{1}{2}\rho U_\infty^2 c))$ is calculated by integrating the pressure distributions around the airfoil, and the drag coefficient $(C_D = D/(\frac{1}{2}\rho U_\infty^2 c))$ is determined by the wake survey method. The uncertainties of the lift and drag coefficients are both estimated to be $(6.3 \times 10^8)Re^{-2}$, which is predicted using the accuracy of the PSI 9816 scanner. Moreover, the uncertainties of the pressure coefficients at each pressure tap have different values for different AOA.
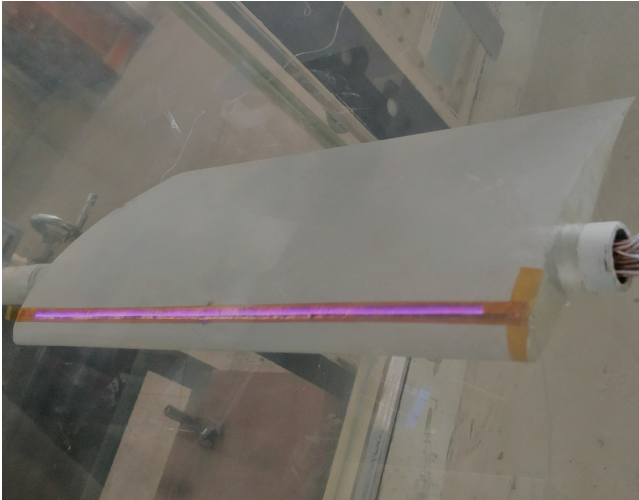
2.2 Dielectric Barrier Discharge Plasma Actuator

As shown in Fig. 3, a 400 mm long strip of dielectric barrier discharge plasma actuator is placed 10% of the chord length from the leading edge of the airfoil. The plasma actuator consists of two asymmetric copper electrodes each of 0.03 mm thickness, among them, the exposed electrode is 2 mm wide and the covered electrode is 4 mm wide. There is no gap or overlap between the exposed and covered electrode. Three layers of Kapton dielectric film (each layer with a thickness of 0.056 mm) are attached between the exposed and the covered electrode, and the whole thickness of the actuator is 0.18 mm [13, 14].
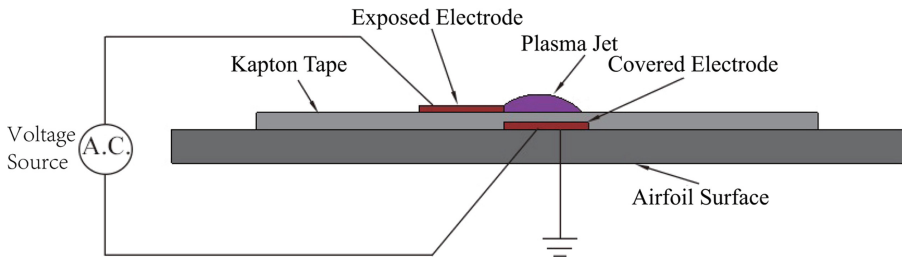

Fig. 3. Dielectric barrier discharge plasma actuator layout sketch

The actuator is connected to a high voltage alternating current (AC) source that provides about 9.0 kV peak-to-peak voltage sinusoidal excitation to the electrodes at a frequency of 9.4 kHz. Furthermore, Fig. 5a shows the AC source's voltage and current traces of time, and Fig. 5b shows the DBD electrical instantaneous power consumption and coupled energy waveforms. Because the manual actuator will affect the boundary layer like a thin trip, three modes of operations of the actuator are defined. The baseline mode corresponds to the case when the actuator is not installed. The plasma-off mode corresponds to the case when the actuator is deactivated. Moreover, the plasma-on mode refers to the conditions when actuator is activated (Fig. 4).

Fig. 4. Dielectric barrier discharge plasma actuator working status

(a)

(b)
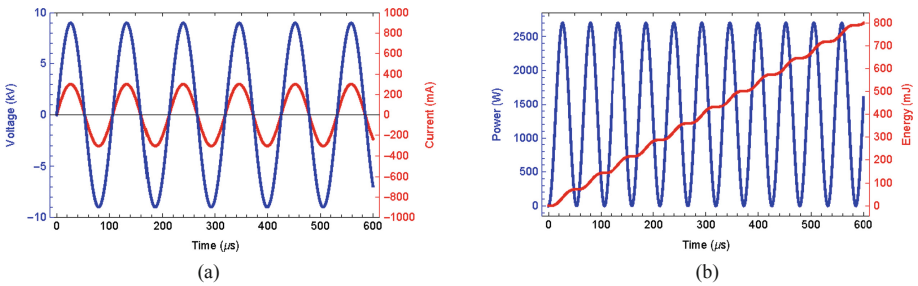
Fig. 5. (a) Voltage and current traces. (b) Instantaneous power and coupled energy waveforms

3 Experimental Results and Discussion

3.1 Baseline Airfoil Characterization

Figure 6a and b separately shows the lift and drag coefficients results of baseline airfoil. The lift and drag measurement results indicate that static hysteresis of the lift and drag occurs on the FX 63-137 airfoil at Reynolds number of 1.8×10^5.

In detail, when $\alpha \leq 14°$, the lift coefficient curves of forward and backward mode are highly consistent, among them, the lift coefficient all reaches the maximum value of 1.5 at $\alpha = 12°$. When the AOA is greater than $14°$, the lift coefficient begins to drop, and the lift coefficient is inconsistent during the forward and backward processes.

An unusual feature of the drag coefficient can also be observed from the Fig. 6b. Similarly, when $Re = 1.8 \times 10^5$, the drag coefficient curves of the forward and backward mode are highly consistent at $\alpha \leq 14°$. As for the medium AOA range $(16° \leq \alpha \leq 20°)$, there is a sharp increase in drag coefficient, and this sudden increase of

the drag coefficient in the forward process is 4°–6° later than the backward. When the AOA is higher than 22°, the drag coefficient becomes the same between the forward and backward process. These results confirm that there exists static hysteresis of drag coefficient at low Reynolds number of 1.8×10^5.
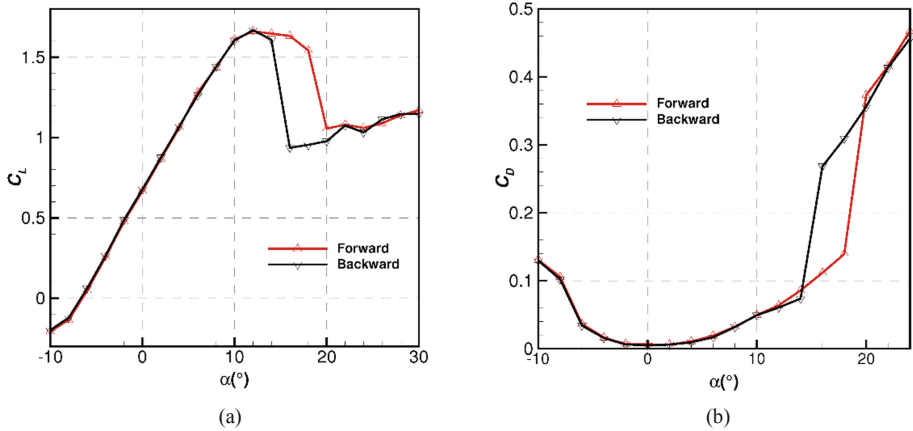

Fig. 6. Lift and drag coefficients change with AOA increase and decrease, $Re = 1.8 \times 10^5$. (a) Lift coefficients change with AOA. (b) Drag coefficients change with AOA

To investigate the physical mechanism of the static hysteresis phenomenon, the pressure measurement results at various AOA are analyzed. The relationship between the laminar separation bubble and pressure distributions was proposed by Mayle [11] in 1991. In the laminar separation bubble region, there is a pressure platform region shown on the pressure distribution graph, which can be used as the criteria for judging the existence of laminar separation bubbles [13].

The pressure distribution results analysis at $Re = 1.8 \times 10^5$ is structured as follows:

- When $-10° \leq \alpha \leq 14°$, the surface pressure distributions in the forward and backward mode are the same. Besides, using the method proposed by Mayle [11], it can be observed that there is a 0.15 c long laminar separation bubble formed on the upper surface of $x/c \approx 0.6$ at $\alpha = 0°$. When $\alpha = 10°$, the separation bubble is found to be formed at $x/c \approx 0.3$, and the separation bubble kept moving upstream on the airfoil at $x/c \approx 0.13$ as the AOA increases to $\alpha = 14°$.
- When $\alpha = 16°, 18°$, the pressure distribution between the forward and backward mode are totally different, which means that the pressure distributions can interpret the static hysteresis of the lift and drag at $\alpha = 16°$ and $18°$.
  - In the forward process, a leading edge separation bubble is formed at $x/c \approx 0.10$, which is presented by a pressure plateau in Fig. 7e. Similarly, in the forward process of $\alpha = 18°$, a separation bubble is formed at $x/c \approx 0.10$, which is also presented by a pressure plateau in Fig. 7f. Then, the flow on the upper surface of the airfoil separated at the neighborhood of $x/c \approx 0.60$.
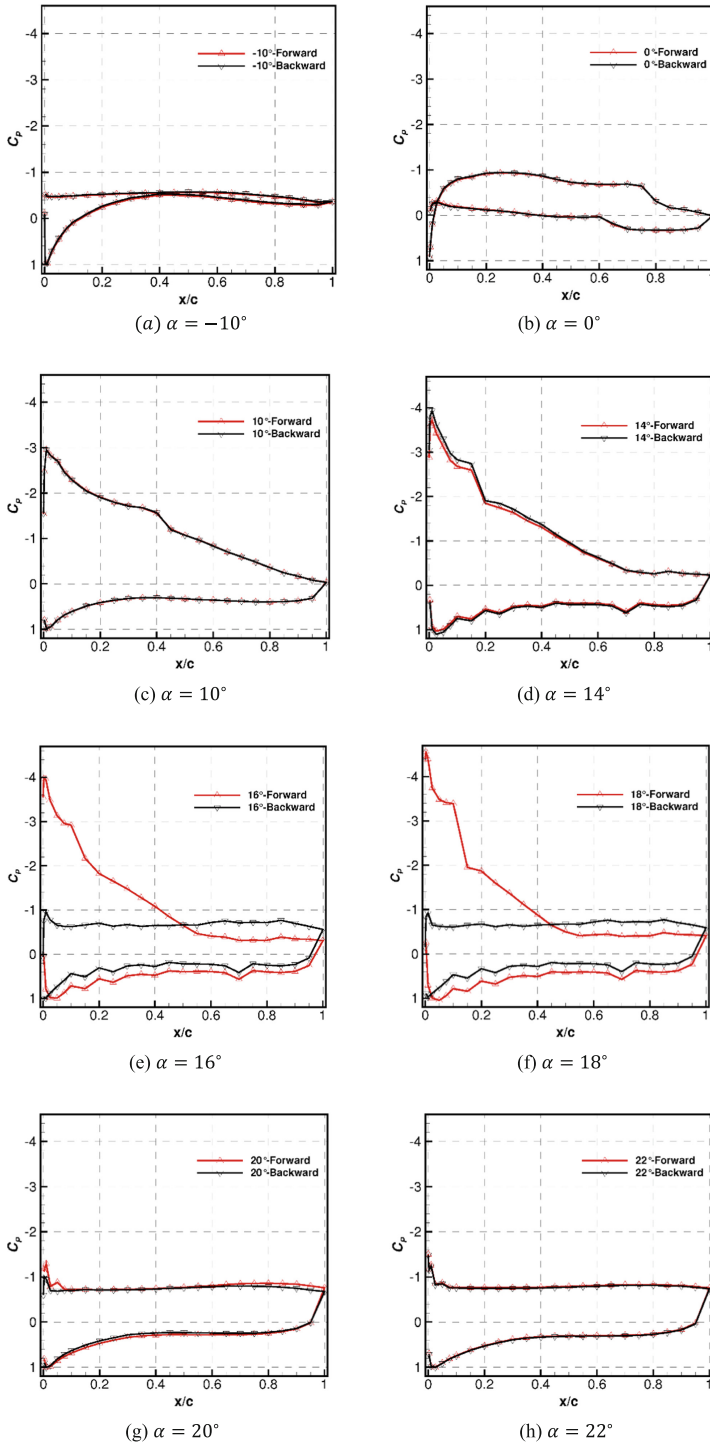
Fig. 7. Surface pressure distributions around the airfoil for baseline condition, $Re = 1.8 \times 10^5$

- – In the backward process, instead of forming a separation bubble on the airfoil surface, the flow over the upper surface of the airfoil separates early from the leading edge, with no reattachment point found. The flow phenomenon described above means a great of lift loss in lift, which accounts for the sharp drop of the lift at $\alpha = 16°$ when $Re = 1.8 \times 10^5$.

- When $\alpha \geq 20°$, in the forward process, the separation bubble bursts and the flow does not reattach after separation, which leads to the sudden drop in the lift coefficient and the increase of the drag coefficient. The flow in the backward process behaves similarly, the flow separates directly from the leading edge, both pressure distributions of the forward and backward process are consistent.

It can be found out that the laminar separation bubble is highly correlated with static hysteresis of the lift and drag. In author's opinion, in forward process, the separation flow reattaches at leading edge of the airfoil and then forms separation bubble, thus, the airfoil has a relatively high lift and low drag. However, in the backward process, the flow on the airfoil has separated and cannot reattaches at the leading edge at the same AOA range, which results in a weaker lift performance. Thus the static hysteresis of lift and drag forms.

3.2 Aerodynamic Characteristics with Plasma Control

Based on the analysis in Sect. 3.1, a further pressure measurement is conducted with the plasma actuator installed at Reynolds number of 1.8×10^5. To avoid the influence of the plasma actuator's geometry, experiments with plasma on and plasma off is conducted. Figure 8a and b separately shows the lift and drag coefficients results of an airfoil with plasma on and off.
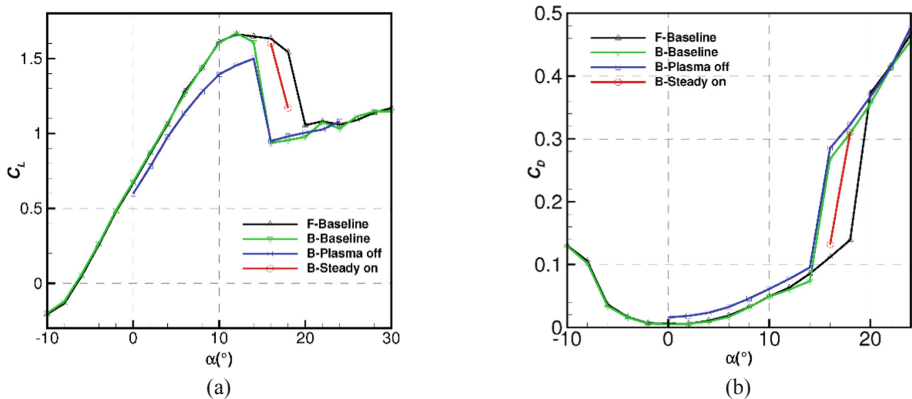
Fig. 8. Comparisons of lift and drag coefficients with and without plasma actuation, $Re = 1.8 \times 10^5$. (a) Comparison of lift coefficients with respect to AOA. (b) Comparison of drag coefficients with respect to AOA
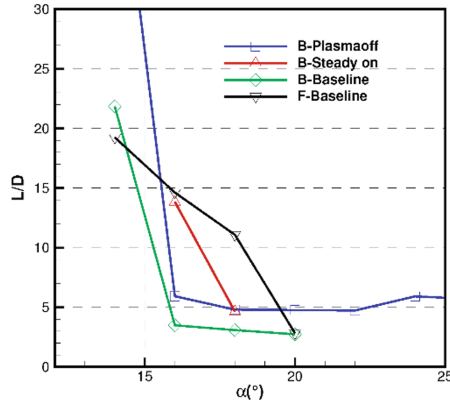
Fig. 9. Comparison of lift-to-drag ratio with respect to AOA without and with plasma actuation, $Re = 1.8 \times 10^5$

As shown in Fig. 8a and b, when $Re = 1.8 \times 10^5$ and $\alpha \geq 20°$, in the backward process, the lift and drag coefficients of the airfoil with actuator installed and the baseline airfoil are almost the same. At the AOA where static hysteresis phenomenon occurs ($\alpha = 16°$ and $\alpha = 18°$), when plasma actuator turned on, the control effect becomes remarkable. In detail, in the backward process, the lift coefficient improved by 19% at $\alpha = 18°$, and the lift coefficient at $\alpha = 16°$ increased by 68.4%. The drag coefficient at $\alpha = 16°$ reduced by 50%, and the drag coefficient at $\alpha = 18°$ keep the same with the backward process. Figure 9 also shows that the lift-to-drag ratios with plasma on at $\alpha = 16°, 18°$ have been improved compared to baseline airfoil. Furthermore, the lift and drag hysteresis has been improved at these AOA with plasma on. It also can be easily concluded from the Fig. 8a that plasma actuator itself has some control effect on lift hysteresis with plasma actuator turned off.

The pressure distributions of the airfoil with and without plasma actuation are presented in Figs. 10 and 11 for clear comparison. Using the same method as Sect. 3.1 to investigate the mechanism of static hysteresis improvement by plasma flow control.

When $Re = 1.8 \times 10^5$ as shown in Figs. 10 and 11, the leading edge separation bubble becomes larger when plasma actuator installed at $\alpha = 16°$, and the peak value of the suction peak is also slightly reduced. In total, the plasma off mode has little effect on the airfoil. When plasma steady on, the plasma actuator induced a leading edge separation bubble at $0.05\ c$ from the leading edge in backward process, and the separation zone shrank, which means that with plasma actuation, the flow separation is adequately controlled. Similarly, when $\alpha = 18°$, in the backward process, the plasma actuator promoted reattachment of separation flow and induced a leading edge separation bubble around $0.1\ c$ from the leading edge of the airfoil, then flow separates again at $0.15\ c$, which indicates that the control effect at $18°$ is not as good as the $16°$ AOA.

(a) Backward

(b) Forward
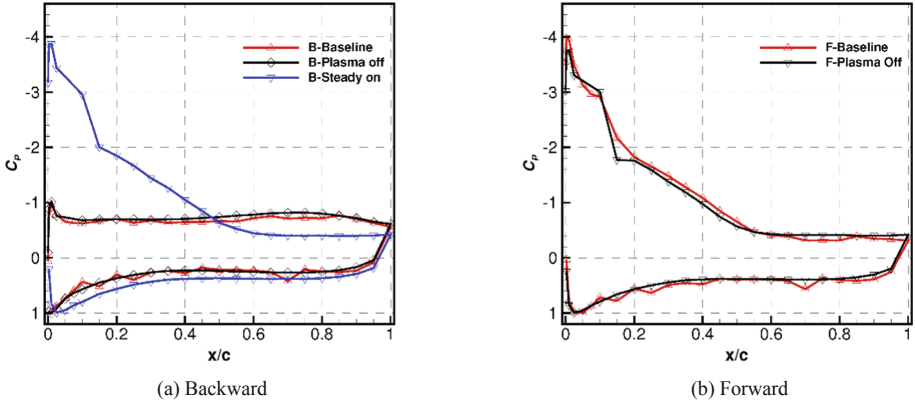
Fig. 10. Surface pressure distributions with plasma on and off, $Re = 1.8 \times 10^5$, $\alpha = 16°$

(a) Backward

(b) Forward
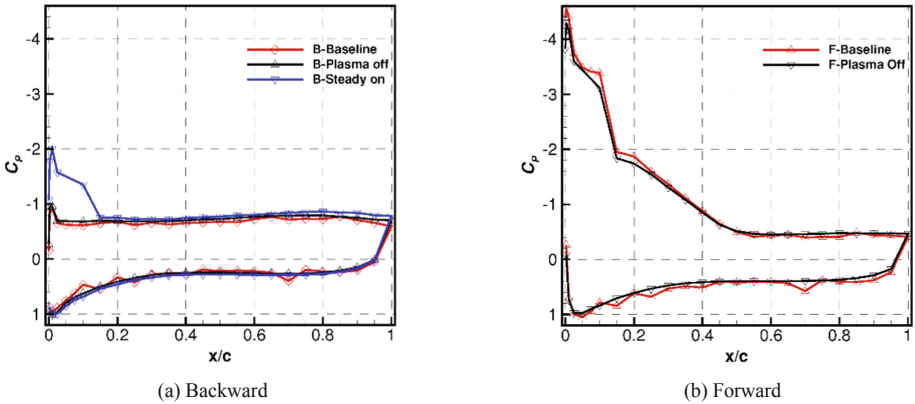
Fig. 11. Surface pressure distributions with plasma on and off, $Re = 1.8 \times 10^5$, $\alpha = 18°$

4   Conclusions

Aerodynamic characteristics of FX 63-137 airfoil at Reynolds number of 1.8×10^5 are studied experimentally. Then, an experiment is carried out to study the plasma flow control effects on static hysteresis at the same Reynolds number. In this experiment, a plasma actuator placed at 10% of chord length from the leading edge of the airfoil is used. The pressure measurements are used to study the underlying physics of static hysteresis on airfoil at low Reynolds numbers.

The lift coefficient curves show that the lift coefficient at small AOA $(\alpha \leq 14°)$ continues to increase at the same Reynolds number, and the slope is a constant. Then, the lift coefficient begins to decrease at medium AOA range $(16° \leq \alpha \leq 20°)$, the lift coefficients of forward and backward process are inconsistent. When $\alpha \geq 22°$, the lift

coefficients of forward and backward process become the same. From the pressure distribution results, it can be concluded that the separation bubble cannot form as the forward process does in the backward process when the stall angle of attack (at $16° \leq \alpha \leq 20°$) has arrived, which resulting in hysteresis of lift and drag in backward process.

The effects of the plasma flow control are as follows: When $Re = 1.8 \times 10^5$, the static hysteresis of lift and drag are significantly improved, the hysteresis of lift and drag is utterly eliminated at $\alpha = 16°$, and the hysteresis of lift and drag is improved at $\alpha = 18°$. In detail, the lift coefficient is increased by 19.2%, and the drag coefficient remained almost the same compared to no control condition. Combining the pressure distribution results and curves of lift and drag coefficients, it can be concluded that the plasma actuator can reduce static hysteresis by promoting the reattachment of leading edge separation flow in backward process.

References

1. Bai P, Cui E, Li F (2006) Study of the nonlinear lift coefficient of the symmetrical airfoil at low Reynolds number near the zero angle of attack. Chin J Theor Appl Mech 38(1):1–8
2. Bai P, Cui E, Zhou W, Li F (2006) Numerical simulation of laminar separation bubble over 2D airfoil at low Reynolds number. Acta Aerodynamica Sinica 24(04):416–424
3. Chen Y, Pan X, Liu Y (2015) Research of the control efficiency of lift increase and drag reduction base on flow around hydrofoil controlled by Lorentz force. Chin J Theor Appl Mech 47(3):414–421. https://doi.org/10.6052/0459-1879-14-346
4. Corke TC, Post ML, Orlov DM (2008) Single dielectric barrier discharge plasma enhanced aerodynamics: physics, modeling and applications. Exp Fluids 46(1):1–26. https://doi.org/10.1007/s00348-008-0582-5
5. Ellsworth RH, Mueller TJ (1991) Airfoil boundary layer measurements at low Re in an accelerating flow from a nonzero velocity. Exp Fluids 11(6):368–374. https://doi.org/10.1007/bf00211791
6. Horton HP (1968) Laminar separation bubbles in two and three dimensional incompressible flow. Thesis
7. Li F, Bai P, Shi W, Li J (2007) Micro air vehicles aerodynamics at low Reynolds number. Adv Mech 37(2):257–268
8. Li Y, Wu Y (2012) Progress of research on plasma flow control technology. J Air Force Eng Univ Nat Sci 3:1–5
9. Liu P, Ma L, Qu Q, Duan Z (2013) Numerical investigation of the laminar separation bubble control by blowing/suction on an airfoil at low Reynolds number. Acta Aerodynamica Sinica 31(4):518–524
10. Liu Q, Bai P, Li F (2017) Aerodynamic characteristics of airfoil and evolution of laminar separation at different Reynolds numbers. Acta Aeronauticaet Astronautica Sinica 38(4): 120,338

11. Mayle RE (1991) The role of laminar-turbulent transition in gas turbine engines. ASME J Turbomach 113(4):509–537. https://doi.org/10.1115/1.2929110
12. Mcgranahan B, Selig M (2003) Surface oil flow measurements on several airfoils at low Reynolds numbers. In: 21st AIAA applied aerodynamics conference, American institute of aeronautics and astronautics. https://doi.org/10.2514/6.2003-4067
13. Meng X, Chen Q, Bai P, Hu H, Yang Z (2016) Laminar separation control at low Reynolds numbers using plasma actuation. Acta Aeronauticaet Astronautica Sinica 37(7):2112
14. Meng X, Hu H, Yan X, Liu F, Luo S (2018) Lift improvements using duty-cycled plasma actuation at low Reynolds numbers. Aerosp Sci Technol 72:123–133. https://doi.org/10.1016/j.ast.2017.10.038
15. Mueller TJ (1985) The influence of laminar separation and transition on low Reynolds number airfoil hysteresis. J Aircraft 22(9):763–770. https://doi.org/10.2514/3.45199
16. Sun Z (2003) Research progress of plasma drag reduction technology. Adv Mech 33(1):87. https://doi.org/10.6052/1000-0992-2003-1-J2001-095
17. Wu J, Li T (2013) Experimental investigation on low Reynolds number behavior of NACA0012 airfoil. J Exp Fluid Mech 27(6):32–38
18. Yang Z, Igarashi H, Martin M, Hu H (2008) An experimental investigation on aerodynamic hysteresis of a low-Reynolds number airfoil. In: 46th AIAA aerospace sciences meeting and exhibit, American institute of aeronautics and astronautics. https://doi.org/10.2514/6.2008-315